

Underwater Terrain and Gravity aided inertial navigation based on Kalman filter

Mohammad Reza Khalilabadi *

* Assistant Professor, Faculty of Naval Aviation, Malek Ashtar University of Technology, Iran;
khalilabadi@mut.ac.ir

ARTICLE INFO

Article History:

Received: 23 Nov. 2020

Accepted: 13 Jan. 2021

Keywords:

Navigation

Underwater

Terrain aided navigation

Gravity aided navigation

Kalman filter

Two maps aided navigation.

ABSTRACT

In this paper, we present a new method for terrain and gravity aided navigation. Gravity aided navigation and terrain aided navigation are map aided navigation methods for correcting Inertial Navigation System (INS) errors of Autonomous Underwater Vehicles (AUV). Map aided navigation uses the information of the geophysical field maps. For achieve the highest accuracy and reliability two or three map aided navigation systems are combined. In this paper, we proposed a new method that simultaneously uses gravity map data and terrain map data. For maps data fusion we use a Kalman filter which its measurement equation defined based on gravity and terrain of the experiment area. The experimental results are encouraging.

1. Introduction

Autonomous Underwater Vehicle (AUV) navigation is widely used to find the location of underwater vehicles that are doing military or commercial applications. According to the underwater environmental characteristics, the electromagnetic waves cannot propagate in the water, so the common navigation systems like the Global Position System (GPS) are not working in the underwater[1–5]. Also using active methods like active sonar may compromise the covertness of underwater vehicles. Therefore the underwater navigation has become an important military and commercial research issue. The inertial navigation system (INS) is commonly used in the autonomous navigation systems which are a navigation technique in which measurements provided by accelerometers and gyroscopes are used to track the position and orientation of a vehicle by using kinematic equations. Since the error of INS is increased over time then the external source is used to update the information of the INS system. Using the information of the geophysical field maps like topography, geomagnetic, and gravity is one of the external information sources[6–9]. The geophysical field maps are digitally stored in the underwater vehicle and one onboard installed sensor repeatedly measures these fields. Comparing field map features and onboard sensor measurements and combine with INS location information can provide accurate vehicle location[10,11]. In some researches [6,12,13] the navigation system is based on matching the measured

positions which are obtained from INS with contours of constant field value of the geophysical maps. In some cases[14–16] the INS information and the field maps information are combined by Bayes filter like Kalman filter for modifying INS system error. To achieve high accuracy and low error navigation systems the information of two or three geophysical maps are combined[17,18,18,18–21]. In this paper, we use gravity and topography maps. The information of two maps is fused with INS information by a Kalman filter which its measurement equation is defined based on gravity and tertian of the experiment area.

In sec.2 we present a survey of Kalman filter which is the data fusion tool in our method. In sec.3 we consider two maps aided navigation systems based on Kalman filter, and in sec.4 the experimental issue and its simulation results are presented and in the last section, the conclusion is presented.

2. Materials and Methods

In signal processing and estimation applications, we encounter some problems that an unknown parameter has appeared in two equations and the Kalman filter has been applied to estimate that parameter by fusion data which obtains of two equations[22–24]. The first equation which called the state equation is modeling the evolving state of parameter and the second equation which called the measurement equation is modeling the relation between the state of parameter and observation of parameter. In the framework of Kalman filter

assume that state equation and measurement equation are linear and the noise distribution is Gaussian. If the unknown parameter in time step k is x_k , then the state equation can be written as:

$$x_k = F_{k-1} \times x_{k-1} + v_{k-1} \quad (1)$$

Where

- x_{k-1} is the previous state
- F_{k-1} is the state transition matrix;
- v_{k-1} is the process noise which is assumed to be a zero mean normal multivariate distribution with covariance Q_{k-1} .

The measurement in time step k , z_k of the state x_k is made according to the measurement equation:

$$z_k = H_k \times x_k + w_k \quad (2)$$

Where

- H_k is the observation matrix
- w_k is the observation noise which is assumed to be a zero mean normal multivariate distribution with covariance R_k .

The Kalman filter is solved in two distinct step: "Prediction" and "Correction" [25]. The prediction step uses the state equation and previous state x_{k-1} to produce an estimation of the state at the current time step, it does not use observation information from the current time step. In the update step, the result of prediction step is combined with current observation information to correct the state estimate. This improved estimate is the output of Kalman filter. If the conditions hold then Kalman filter equation can be written as follow:

Prediction step:

$$x_{k|k-1} = F_{k-1} \times x_{k-1} \quad (3)$$

$$P_{k|k-1} = Q_{k-1} + F_{k-1} P_{k-1} F_{k-1}^T$$

Correction step:

$$x_k = x_{k|k-1} + K_k (z_k - H_k x_{k|k-1}) \quad (4)$$

$$P_k = (I - K_k H_k) P_{k|k-1} \quad (5)$$

Where the K_k is Kalman gain and can be obtained as

$$K_k = P_{k|k-1} H_k (H_k P_{k|k-1} H_k^T + R_k)^{-1} \quad (6)$$

Two Maps Aided Navigation

Two maps aided navigation method uses the information of two geophysical maps to the improved output of INS navigation system. Information that comes from two geophysical maps and information of the INS navigation system is combined by the Kalman filter. The navigation state vector is defined

$$X = \begin{bmatrix} x \\ y \\ v_x \\ v_y \end{bmatrix} \quad (7)$$

Where the x and y are coordinates of underwater vehicle, v_x and v_y are velocity of vehicle in directions of this coordinate axes. The INS state vector is denoted by X_k^* , which is include location and velocity of underwater vehicle. The real vector state of underwater vehicle is denoted by X_k . The error vector state δX_k is defined as follow:

$$\delta X_k = X_k - X_k^* = \begin{bmatrix} x - x^* \\ y - y^* \\ v_x - v_x^* \\ v_y - v_y^* \end{bmatrix} = \begin{bmatrix} \delta x \\ \delta y \\ \delta v_x \\ \delta v_y \end{bmatrix} \quad (8)$$

In fact, δX_k is the INS error in time step k [7,26,27]. in two maps aided navigation system the error vector is considered as the state parameter of the Kalman filter. As discussed earlier for applying the Kalman filter to a problem we need two equations, the state equation, and the measurement equation. By considering the error vector as the state parameter of the Kalman filter it can be shown that state equation can be written:

$$\delta X_k = \begin{bmatrix} 1 & 0 & \tau & 0 \\ 0 & 1 & 0 & \tau \\ 0 & 0 & 1 & 0 \\ 0 & 0 & 0 & 1 \end{bmatrix} \delta X_{k-1} + V_k \quad (9)$$

Where τ is the duration of the one timestep and v_k is the process noise which is assumed to be a zero-mean Gaussian distribution with covariance Q_k . The state equation can be written as follow:

$$\delta X_k = \Phi(\tau) \delta X_{k-1} + V_k \quad (10)$$

In the map aided navigation, the measurement of vehicle state is generated by a sensor that installed in the vehicle. The measurement according to the field maps can be gravity, terrain, or geomagnetic. Another measurement of the vehicle state can be generated by referring to the fields map. INS system coordinates of vehicle can be found on the map and its equivalent field amount is the measurement. in map aided navigation when the Kalman filter is applied, the measurement is defined as the difference between the sensor measurement and the map referenced measurement [28,29]. If g_1 and g_1^* denote sensor and map reference measurement for first map and If g_2 and g_2^* denote sensor and map reference measurement for the second

map then measurement equation for the two maps aided navigation can be written:

$$z = \begin{bmatrix} \delta g_1 \\ \delta g_2 \end{bmatrix} = \begin{bmatrix} g_1 - g_1^* \\ g_2 - g_2^* \end{bmatrix} = \begin{bmatrix} h_{x1} & h_{y1} & 0 & 0 \\ h_{x2} & h_{y2} & 0 & 0 \end{bmatrix} \begin{bmatrix} x - x^* \\ y - y^* \\ v_x - v_x^* \\ v_y - v_y^* \end{bmatrix} + W_k \quad (11)$$

Where W_k is the observation noise which is assumed to be a zero mean Gaussian distribution with covariance R_k . The surface of the maps are assumed to be plane shape in vicinity of (x^*, y^*) and h_{x1} , h_{y1} , h_{x2} and h_{y2} are slopes of the two planes. Generally the plane equation has the bellow form:

$$f(x, y) = a + h_x(x - x^*) + h_y(y - y^*) \quad (12)$$

Where the h_x and h_y are horizontal and vertical slopes of the plane. Due to the definition of state vector δX_k the measurement equation can be written as follow.

$$z_k = H_k \times \delta X_k + W_k \quad (13)$$

As mentioned in the previous part, Kalman filter is applied for the problems that have two linear equations with Gaussian noise. It is seen that the two maps aided navigation issue has the Kalman filter framework so that can be applied. By using the Kalman filter equations (3)-(6), the navigation problem equation can be obtained.

State and covariance in the prediction step become

$$\delta X_{k|k-1} = \Phi(\tau)\delta X_{k-1} \quad (14)$$

$$P_{k|k-1} = \Phi(\tau)P_{k-1}\Phi^T(\tau) + Q_k \quad (15)$$

State and covariance in the update step become

$$\delta X_k = \delta X_{k|k-1} + K_k (g_k - H_k \delta X_{k|k-1}) \quad (16)$$

$$P_k = (I - H_k K_k) P_{k|k-1} \quad (17)$$

Where the g_k is the measurement vector and the K_k is Kalman gain that is given by

$$K_k = P_{k|k-1} H_k^T (H_k P_{k|k-1} H_k^T + R_k)^{-1} \quad (18)$$

After the error state vector δX_k was estimated in (16), the real state of the underwater can be obtained by

$$X_k = X_k^* + \delta X_k \quad (19)$$

4. Results and Discussion

In order to test the accuracy and performance of the proposed method, experiments with real data were carried out. Field maps are topography and gravity with '1*1' latitude-longitude resolution. The maps as shown in figure (1) have been taken of the Gulf of Oman in the Middle East (red rectangular). In recent years, a lot of research has been done on the environmental characteristics and waters of this region[30–34].

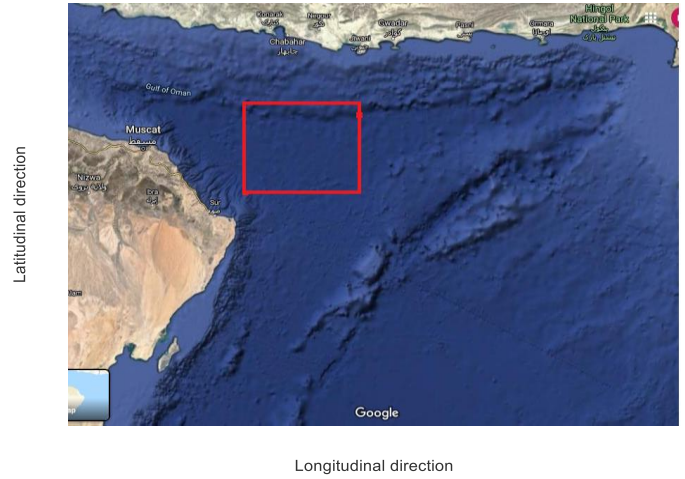


Figure 1. Study area in the Gulf of Oman

The Three-dimensional terrain and gravity maps of the experiment area are shown in figure (2). For the gravity map, we subtracted gravity value by the constant 9.8 and multiplied by 1000.

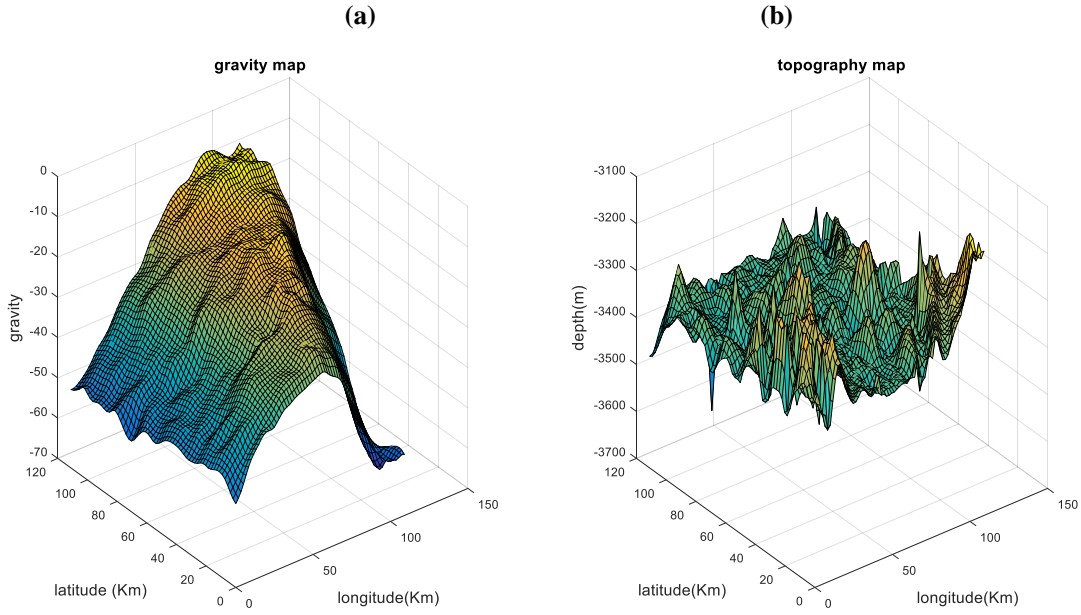


Figure 2. (a): 3-D gravity map, (b): 3-D terrain map of the study area

Suppose a vehicle that was in position (0,0) of the experiment area started its mission. The vehicle travels with a speed of 3 Km/h in the longitudinal direction and 4 Km/h in the latitudinal direction. For noise covariance in the state and measurement equation we have

$$Q_k = \begin{bmatrix} 1 & 0 & 0 & 0 \\ 0 & .1 & 0 & 0 \\ 0 & 0 & 1 & 0 \\ 0 & 0 & 0 & .1 \end{bmatrix}$$

$$R_k = \begin{bmatrix} .2 & 0 \\ 0 & .2 \end{bmatrix}$$

The timestep τ is considered 1 h and so the transition matrix become

$$\Phi(\tau) = \begin{bmatrix} 1 & 0 & 1 & 0 \\ 0 & 1 & 0 & 1 \\ 0 & 0 & 1 & 0 \\ 0 & 0 & 0 & 1 \end{bmatrix}$$

Geophysical maps are a nonlinear function of position and commonly stored as a square grid of field values. Therefore, the observation matrix H_k is obtained by linearization of the maps. As mentioned in sec.3 the field maps must be a plane surface which is a linear expression of filed value and positions. So for calculating the H_k , a plane surface is fitted to a small area in the nearby of the INS navigated position. For example, the small area of the topography map and its equivalent plane surface is shown in the figure (3). the

equivalent plane surface is obtained by using linear regression techniques or neural network [35–38].

After obtaining the equivalent linear plane the elements of matrix H_k which are slopes of the equivalent planes can be obtained.

The absolute position error (Km) of these methods is shown in Figure (4). It can be seen from figure (4) that INS position error increase with time and it is shown that the proposed method has the lowest error level, subsequently the INS position errors can be corrected effectively by applying this method. The error of the two other navigation methods the gravity-map aided navigation and topography-map aided navigation is more than error of two maps aided navigation. Filed maps always do not have valid information, for example, the topography map in flat areas doesn't have valid information for the navigation systems, or some paths have the almost same field values so the navigation system may be confused which paths is the real path of the vehicle and navigation systems may not convergence to real position. In the table (1) we do 10000 runs of the navigation methods in this paper. This table shows that two maps aided navigation has the highest valid navigation probability.

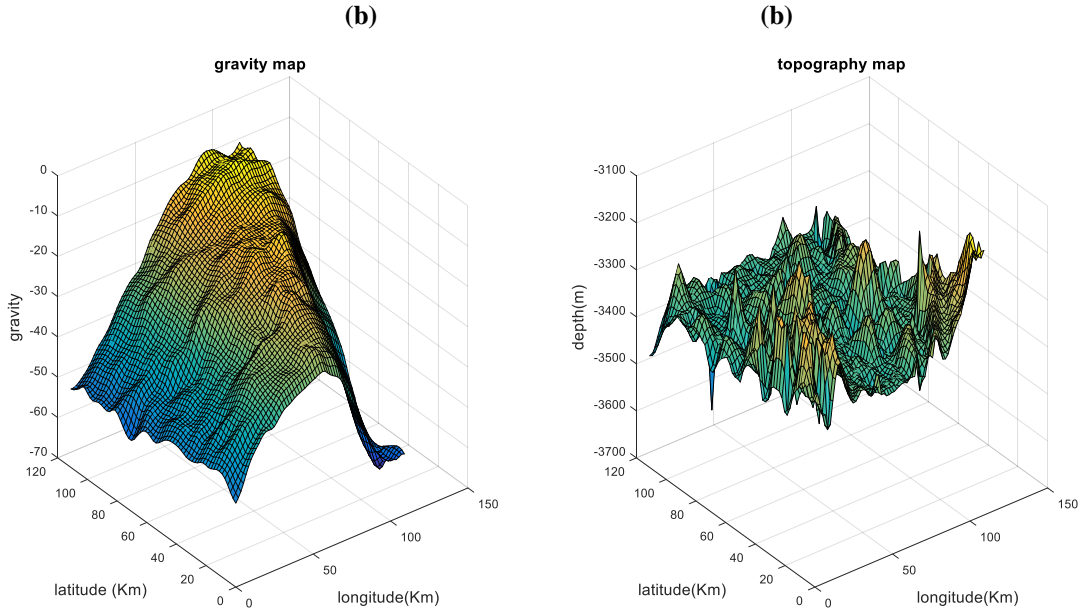


Figure 2. (a): 3-D gravity map, (b): 3-D terrain map of the study area

Table 1. Valid navigation probability or convergence probability

Navigation method	convergence probability
Gravity aided navigation	%79
Terrain aided navigation	%75
Two maps aided navigation	%99.8

5. Conclusions

We presented a method for underwater vehicle navigation by measuring gravity and terrain of the water. The Kalman filter is used to combining information that comes from maps, sensors, and INS. The results show this method has high accuracy more than other methods and have high valid navigation probability. Two maps aided navigation method that presented in this paper does navigation based one filtering stage, unlike the other two maps aided method which uses one Kalman filter for every map and so the valid navigation probability can be decreased.

List of Symbols

K_k	Kalman gain
w_k	observation noise
H_k	observation matrix
v_x and v_y	velocity components of vehicle
v_k	process noise
g_k	measurement vector

6. References

- Paull, L., S. Saeedi, M. Seto and H. Li, 2013. AUV navigation and localization: A review. *IEEE Journal of Oceanic Engineering*, 39(1): 131–149.
- Allotta, B., A. Caiti, R. Costanzi, F. Fanelli, D. Fenucci, E. Meli and A. Ridolfi, 2016. A new AUV navigation system exploiting unscented Kalman filter. *Ocean Engineering*, 113: 121–132.
- Mu, X., J. Guo, Y. Song, Q. Sha, J. Jiang, B. He and T. Yan, 2017. Application of modified EKF algorithm in AUV navigation system, In *OCEANS 2017-Aberdeen*, IEEE, pp: 1–4.
- Salavasidis, G., A. Munafo, C.A. Harris, S.D. McPhail, E. Rogers and A.B. Phillips, 2018. Towards arctic AUV navigation. *IFAC-PapersOnLine*, 51(29): 287–292.
- Franchi, M., A. Ridolfi and M. Pagliai, 2020. A forward-looking SONAR and dynamic model-based AUV navigation strategy: Preliminary validation with FeelHippo AUV. *Ocean Engineering*, 196: 106770.
- Kamgar-Parsi, B. and B. Kamgar-Parsi, 1999. Vehicle localization on gravity maps, In *Unmanned Ground Vehicle Technology*, International Society for Optics and Photonics, pp: 182–191.
- Wu, L., J. Ma and J. Tian, 2010. A self-adaptive unscented Kalman filtering for underwater gravity aided navigation, In *IEEE/ION Position, Location and Navigation Symposium*, IEEE, pp: 142–145.
- Wang, H., L. Wu, H. Chai, H. Hsu and Y. Wang, 2016. Technology of gravity aided inertial

- navigation system and its trial in South China Sea. *IET Radar, Sonar & Navigation*, 10(5): 862–869.
9. Kuang, J., X. Niu, P. Zhang and X. Chen, 2018. Indoor positioning based on pedestrian dead reckoning and magnetic field matching for smartphones. *Sensors*, 18(12): 4142.
 10. Li, M., Y. Liu and L. Xiao, 2014. Performance of the ICCP algorithm for underwater navigation, In 2014 International Conference on Mechatronics and Control (ICMC), IEEE, pp: 361–364.
 11. Wang, H., X. Xu and T. Zhang, 2018. Multipath parallel ICCP underwater terrain matching algorithm based on multibeam bathymetric data. *IEEE Access*, 6: 48708–48715.
 12. Bishop, G.C., 2002. Gravitational field maps and navigational errors [unmanned underwater vehicles]. *IEEE Journal of Oceanic Engineering*, 27(3): 726–737.
 13. Zhang, H., L. Yang and M. Li, 2019. Improved ICCP algorithm considering scale error for underwater geomagnetic aided inertial navigation. *Mathematical Problems in Engineering*, 2019:.
 14. Wu, M. and J. Yao, 2015. Adaptive UKF-SLAM based on magnetic gradient inversion method for underwater navigation, In 2015 International Conference on Unmanned Aircraft Systems (ICUAS), IEEE, pp: 839–843.
 15. Melo, J. and A. Matos, 2017. Survey on advances on terrain based navigation for autonomous underwater vehicles. *Ocean Engineering*, 139: 250–264.
 16. Bozorg, M., M.S. Bahraini and A.B. Rad, 2019. New Adaptive UKF Algorithm to Improve the Accuracy of SLAM. *International Journal of Robotics, Theory and Applications*, 5(1): 35–46.
 17. Deng, Z., Y. Ge, W. Guan and K. Han, 2010. Underwater map-matching aided inertial navigation system based on multi-geophysical information. *Frontiers of Electrical and Electronic Engineering in China*, 5(4): 496–500.
 18. Zheng, H., H. Wang, L. Wu, H. Chai and Y. Wang, 2013. Simulation research on gravity-geomagnetism combined aided underwater navigation. *The Journal of Navigation*, 66(1): 83–98.
 19. Wang, H., L. Wu, H. Chai, Y. Xiao, H. Hsu and Y. Wang, 2017. Characteristics of marine gravity anomaly reference maps and accuracy analysis of gravity matching-aided navigation. *Sensors*, 17(8): 1851.
 20. Wang, C., B. Wang, Z. Deng and M. Fu, 2020. A Delaunay Triangulation Based Matching Area Selection Algorithm for Underwater Gravity-Aided Inertial Navigation. *IEEE/ASME Transactions on Mechatronics*.
 21. Bao, J., D. Li, X. Qiao and T. Rauschenbach, 2020. Integrated navigation for autonomous underwater vehicles in aquaculture: A review. *Information Processing in Agriculture*, 7(1): 139–151.
 22. Michalski, J., P. Koziński and J. Ziętkiewicz, 2019. The new approach to hybrid Kalman filtering, based on the changed order of filters for state estimation of dynamical systems. *Poznan University of Technology Academic Journals. Electrical Engineering*.
 23. Cummins, D.P., D.B. Stephenson and P.A. Stott, 2020. A new energy-balance approach to linear filtering for estimating effective radiative forcing from temperature time series. *Advances in Statistical Climatology, Meteorology and Oceanography*, 6(2): 91–102.
 24. Meslem, N. and N. Ramdani, 2020. A new approach to design set-membership state estimators for discrete-time linear systems based on the observability matrix. *International Journal of Control*, 93(11): 2541–2550.
 25. Masnadi-Shirazi, H., A. Masnadi-Shirazi and M.-A. Dastgheib, 2019. A Step by Step Mathematical Derivation and Tutorial on Kalman Filters. *ArXiv Preprint ArXiv:1910.03558*.
 26. Wu, L., H. Wang, H. Chai, H. Hsu and Y. Wang, 2015. Research on the relative positions-constrained pattern matching method for underwater gravity-aided inertial navigation. *The Journal of Navigation*, 68(5): 937–950.
 27. Wei, E., C. Dong, J. Liu, Y. Yang, S. Tang, G. Gong and Z. Deng, 2017. A robust solution of integrated SITAN with TERCOM algorithm: weight-reducing iteration technique for underwater vehicles' gravity-aided inertial navigation system. *NAVIGATION, Journal of the Institute of Navigation*, 64(1): 111–122.
 28. Wu, L., J. Gong, H. Cheng, J. Ma and J. Tian, 2007. New method of underwater passive navigation based on gravity gradient, In *MIPPR 2007: Remote Sensing and GIS Data Processing and Applications; and Innovative Multispectral Technology and Applications*, International Society for Optics and Photonics, p: 67901V.
 29. Wu, L. and J. Tian, 2010. Automated gravity gradient tensor inversion for underwater object detection. *Journal of Geophysics and Engineering*, 7(4): 410–416.
 30. Mashayekhpour, M., R. Emadi and M. Torabi Azad, 2018. Investigation on the Seasonal Variations of Tidal Constituents in the North Coasts of Persian Gulf and Oman Sea. *Hydrophysics*, 2(2): 67–77.
 31. Hosseini hamid, M. and M. Akbarinasab, 2016. The Calculation of the Optimum Index Factor for Monitoring Water Resources pollution using Satellite Images: A Case Study of the Oman sea. *Hydrophysics*, 2(1): 35–45.
 32. ghazi, E., M. Ezam, A. Aliakbari Bidokhti, M. Torabi Azad and E. Hasanzade, 2018. Modeling

- Thermohaline Front of the Persian Gulf Outflow in the Oman Sea. *Hydrophysics*, 4(1): 1–17.
33. yazdanfar, salar, A. Amir Ashtari Larki, mohammad akbarinasab and A. Delbari, 2018. Study of surface fronts in the Oman Sea. *Hydrophysics*, 4(1): 19–31.
 34. rahnemania, abdossamad, A.A. Aliakbari Bidokhti, M. Ezam, K. Lari and S. Ghader, 2019. The Role of Bottom Friction on the Changes of Salinity Front in the Persian Gulf. *Hydrophysics*, 4(2): 15–25.
 35. Lubis, F.F., Y. Rosmansyah and S.H. Supangkat, 2014. Gradient descent and normal equations on cost function minimization for online predictive using linear regression with multiple variables, In 2014 International Conference on ICT For Smart Society (ICISS), IEEE, pp: 202–205.
 36. Shanthamallu, U.S., A. Spanias, C. Tepedelenlioglu and M. Stanley, 2017. A brief survey of machine learning methods and their sensor and IoT applications, In 2017 8th International Conference on Information, Intelligence, Systems & Applications (IISA), IEEE, pp: 1–8.
 37. Pillai, A.S., G.S. Chandraprasad, A.S. Khwaja and A. Anpalagan, 2019. A service oriented IoT architecture for disaster preparedness and forecasting system. *Internet of Things*, 100076.
 38. Singh, S. and M. St-Hilaire, 2020. Prediction-Based Resource Assignment Scheme to Maximize the Net Profit of Cloud Service Providers. *Communications and Network*, 12(02): 74.